Complementary Astrophysics

L8 - The ISM (Behind the Scenes)

What did we learn?

What did we learn?

1. What is the ISM

2. Type of clouds

3. Molecular component of the ISM

4. Neutral component of the ISM

5. Dust component of the ISM

6. Stars-ISM relation

Outline of the course

1. History
2. Review of the general concepts
3. Galaxies in our local Universe
4. Galaxies kinematics
5. Scaling relations
6. Star formation
7. Interstellar Medium
8. **Interstellar Medium – Behind the Scenes**

SFR – Gas fraction

Gas fraction = Gas mass-total mass ratio (total mass includes stars and dark matter).
SFR = Proxy of the rate at which gas is being converted into stars.

Galaxies need gas to form new stars → more gas = higher probability for star formation

N.B. = Gas is a necessary but not sufficient condition for star formation.

The dependence of SFR and the gas fraction in galaxies is seen in the Kennicutt-Schmidt law,
KS law = SFR density proportional to the gas density (to a power of about 1.4)

$$SFR \propto \Sigma^{1.4}(HI+H2)$$

N.B. = A galactic bulge or an AGN can also affect the SFR
and gas fraction in a galaxy.
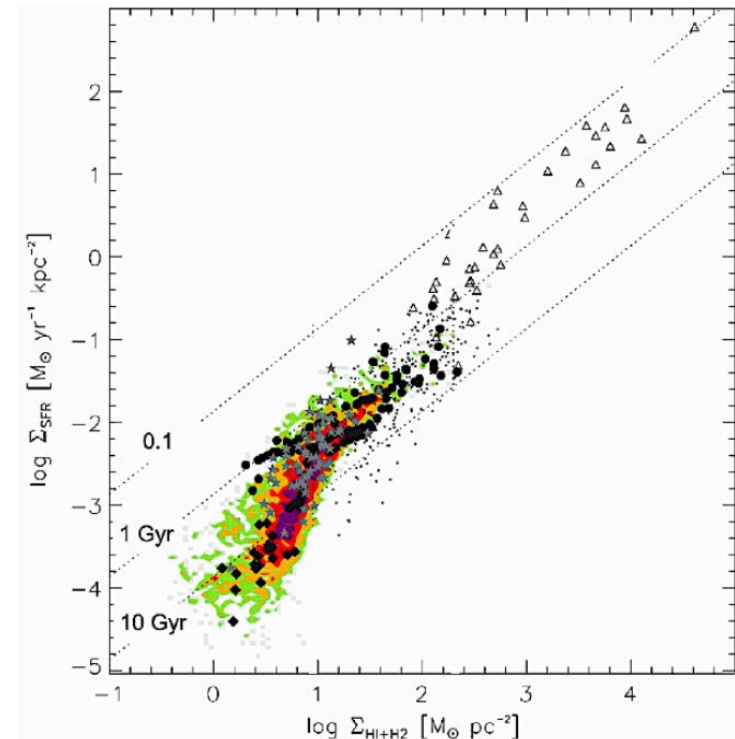
How does evolve the gas fraction with z?

SFR – Gas fraction

~90% of the SFR lies in normal star-forming galaxies: Main Sequence.
- The main sequence evolve with redshift, with main sequence SFR at a given M_* increasing with z, because of the rise of the specific SFR of galaxies from present-time to the peak of the cosmic star formation.
- The molecular gas fraction also increase with z: galaxies are usually ordered disc rotationally supported. The main problem is that they are highly turbulent with high average velocity dispersion
→ marginally stable discs, contrary to their local counterparts.

Magnelli+20

SFR – Gas fraction
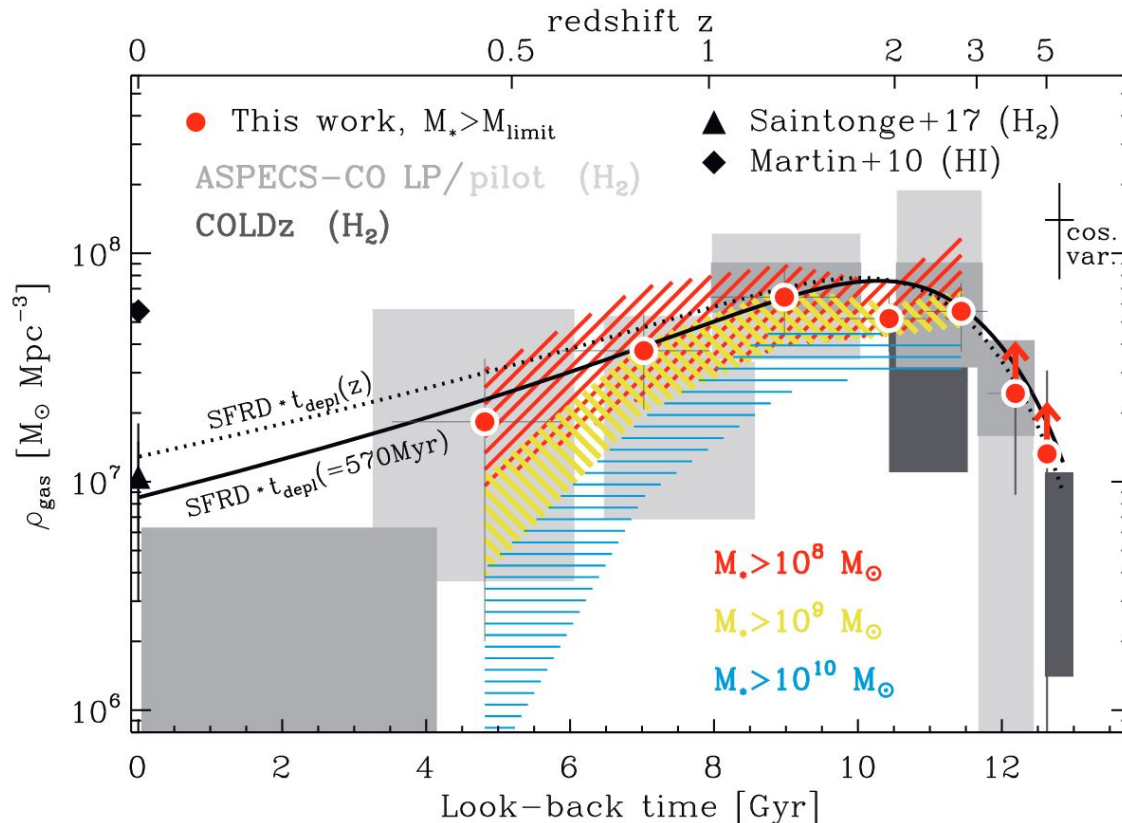
The ALMA Reionization Era Bright Emission Line Survey

The molecular gas content of galaxies at $z \sim 7$

M. Aravena[1], K. Heintz[2,3], M. Dessauges-Zavadsky[4], P. Oesch[2,3,4], H. Algera[5,6], R. Bouwens[7], E. Da Cunha[8], P. Dayal[9], I. De Looze[10], A. Ferrara[11], Y. Fudamoto[6,12], V. Gonzalez[13], L. Graziani[14,15], H. Inami[5], A. Pallottini[11], R. Schneider[14,15,16,17], S. Schouws[7], L. Sommovigo[14], M. Topping[18], P. van der Werf[7], and M. Palla[10]

ABSTRACT

A key to understanding the formation of the first galaxies is to quantify the content of the molecular gas as the fuel for star formation activity through the epoch of reionization. In this paper, we use the $158\mu m$ [C II] fine-structure emission line as a tracer of the molecular gas in the interstellar medium (ISM) in a sample of $z = 6.5 - 7.5$ galaxies recently unveiled by the Reionization Era Bright Line Emission Survey, REBELS, with the Atacama Large Millimeter/submillimeter Array. We find substantial amounts of molecular gas ($\sim 10^{10.5} M_\odot$) comparable to those found in lower redshift galaxies for similar stellar masses ($\sim 10^{10} M_\odot$). The REBELS galaxies appear to follow the standard scaling relations of molecular gas to stellar mass ratio (μ_{mol}) and gas depletion timescale (t_{dep}) with distance to the star-forming main-sequence expected from extrapolations of $z \sim 1 - 4$ observations. We find median values at $z \sim 7$ of $\mu_{mol} = 2.6^{4.1}_{-1.4}$ and $t_{dep} = 0.5^{+0.26}_{-0.14}$ Gyr, indicating that the baryonic content of these galaxies is gas-phase dominated and little evolution from $z \sim 7$ to 4. Our measurements of the cosmic density of molecular gas, $\log(\rho_{mol}/(M_\odot Mpc^{-3})) = 6.34^{+0.34}_{-0.31}$, indicate a steady increase by an order of magnitude from $z \sim 7$ to 4.

Key words. galaxies: evolution – galaxies: high-redshift – galaxies: ISM – ISM: molecules

SFR – Gas fraction

**Ciências
ULisboa**

Magnelli+20

Aravena+23
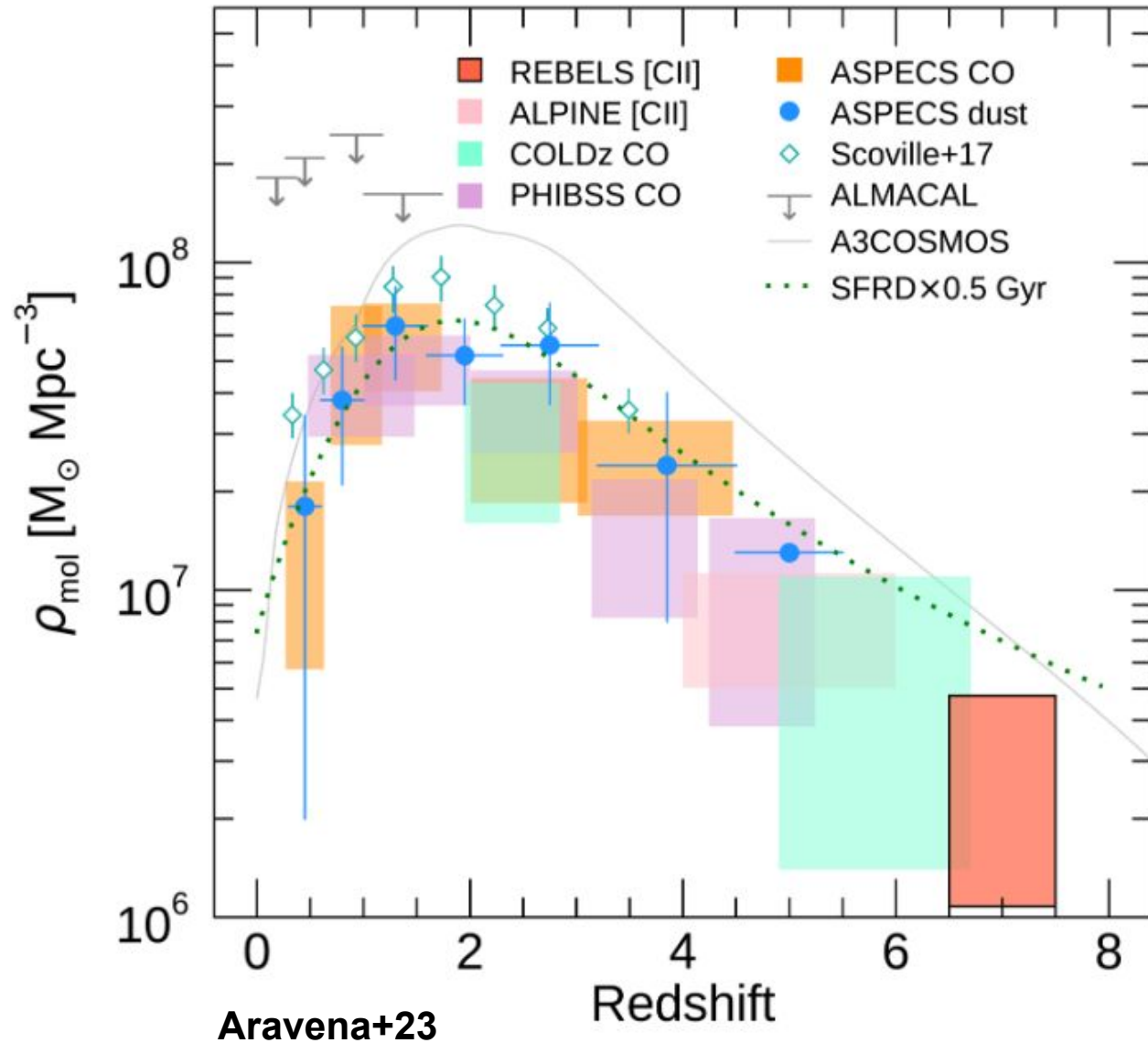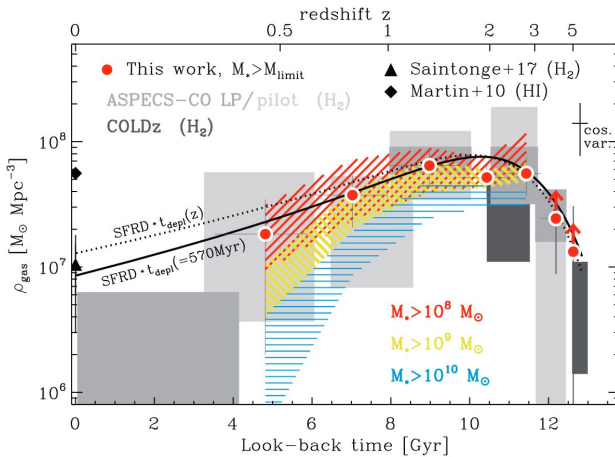
SFR – Gas fraction

Galaxies tend to have higher gas fractions and higher SFRs compared to galaxies in the local universe.
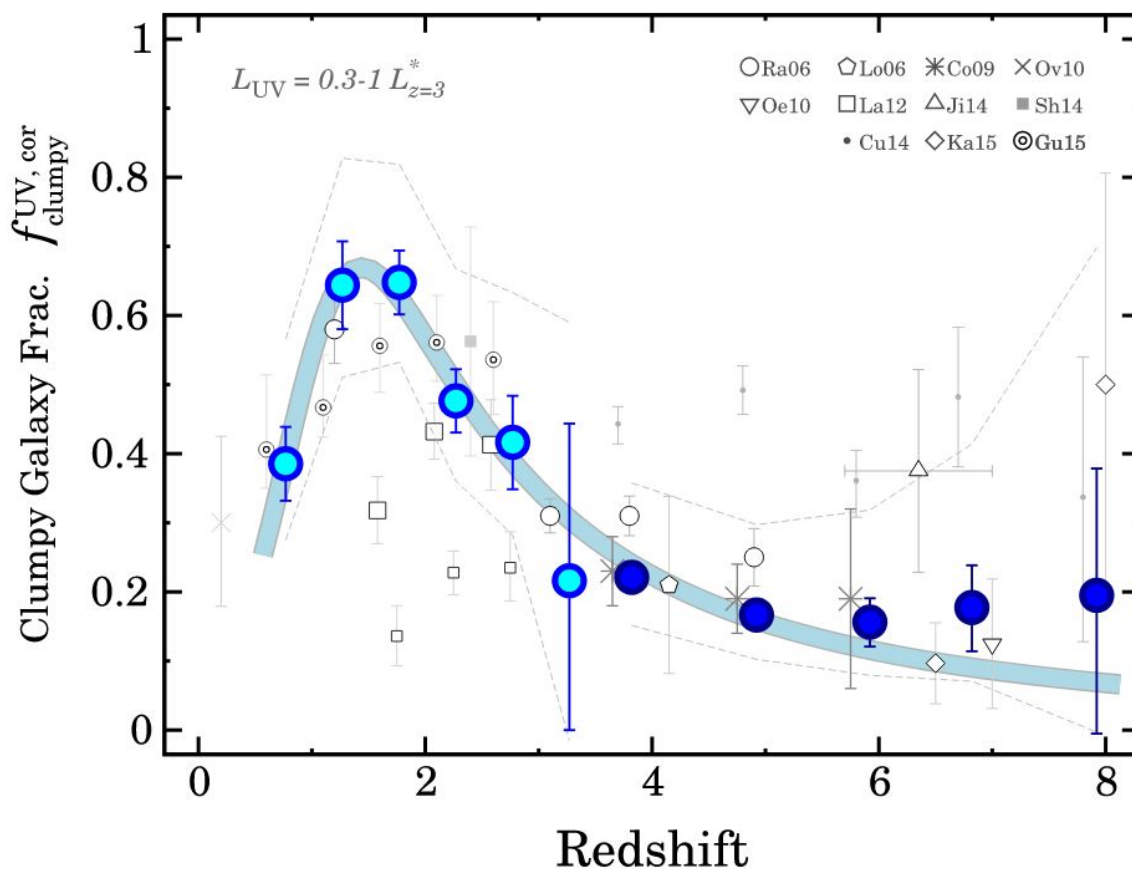
Why?

Galaxies at high-z are still forming and accreting gas; no gas depletion due to star formation (cosmic noon)

How does it evolve the morphology (clumpiness) of the Universe?

Galaxies at the peak of SFH have clumpy, irregular morphologies, with median masses of 10^7 M$_o$, SFR > 0.5 M$_o$/yr and sizes ~30–300 pc.

Figure 4. Redshift evolution of the clumpy galaxy fraction, $f_{clumpy}^{UV,cor}$, at $z \simeq 0$–8 for the star-forming galaxies with $L_{UV} = 0.3$–$1L_{z=3}^*$. The filled cyan and blue circles denote the SFGs and the LBGs, respectively. The error bars are given by Poisson statistics from the galaxy number counts. The cyan solid curve denotes the best-fit formula of Equation (3) (Madau & Dickinson 2014). The gray dashed lines present the upper and lower limits of $f_{clumpy}^{UV,cor}$ derived by changing F_c in a range of $0.5 \times F_c^{fid} - 2 \times F_c^{fid}$, where F_c^{fid} is the fiducial F_c value for each redshift. The gray symbols show LBAs and LBGs with clumps or irregular morphologies in the literature (open circles: Ravindranath et al. 2006; pentagon: Lotz et al. 2006; asterisks: Conselice & Arnold 2009; inverse triangle: Oesch et al. 2010; cross: Overzier et al. 2010; open squares: Law et al. 2012a; triangle: Jiang et al. 2013; filled square: Shibuya et al. 2014; diamonds: Kawamata et al. 2015; dots: Curtis-Lake et al. 2014). The small and large open squares are based on the selection of clumpy galaxies with the GM_{20} and A indices, respectively. The double circles represent $f_{clumpy}^{UV,cor}$ for SFGs with $\log M_*/M_\odot = 9.6$–10.4 in Guo et al. (2015). The error bars are given by Poisson statistics from the number of sample galaxies, if no error bar has been presented in the literature.

Shibuya+16

SF evolution

Galaxies at the peak of SFH have clumpy, irregular morphologies, with median masses of 10^7 M$_o$, SFR > 0.5 M$_o$/yr and sizes ~30–300 pc (Shibuya+16).

The Stellar Mass and Age Distributions of Star-Forming Clumps at $0.5 < z < 5$ in JWST CANUCS: Implications for Clump Formation and Destruction

VISAL SOK [1], ADAM MUZZIN [1], VIVIAN YUN YAN TAN [1], YOSHIHISA ASADA [2,3], MARUŠA BRADAČ [4,5]
VINCE ESTRADA-CARPENTER [6,7,8], KARTHEIK G. IYER [9,10], NICHOLAS S. MARTIS [4], GAËL NOIROT [11]
GHASSAN T. E. SARROUH [1], MARCIN SAWICKI [8], CHRIS J. WILLOTT [12], SUNNA WITHERS [1]
SAMANTHA C. BEREK [13,2,14] AND KATHERINE MYERS [1]

SF evolution
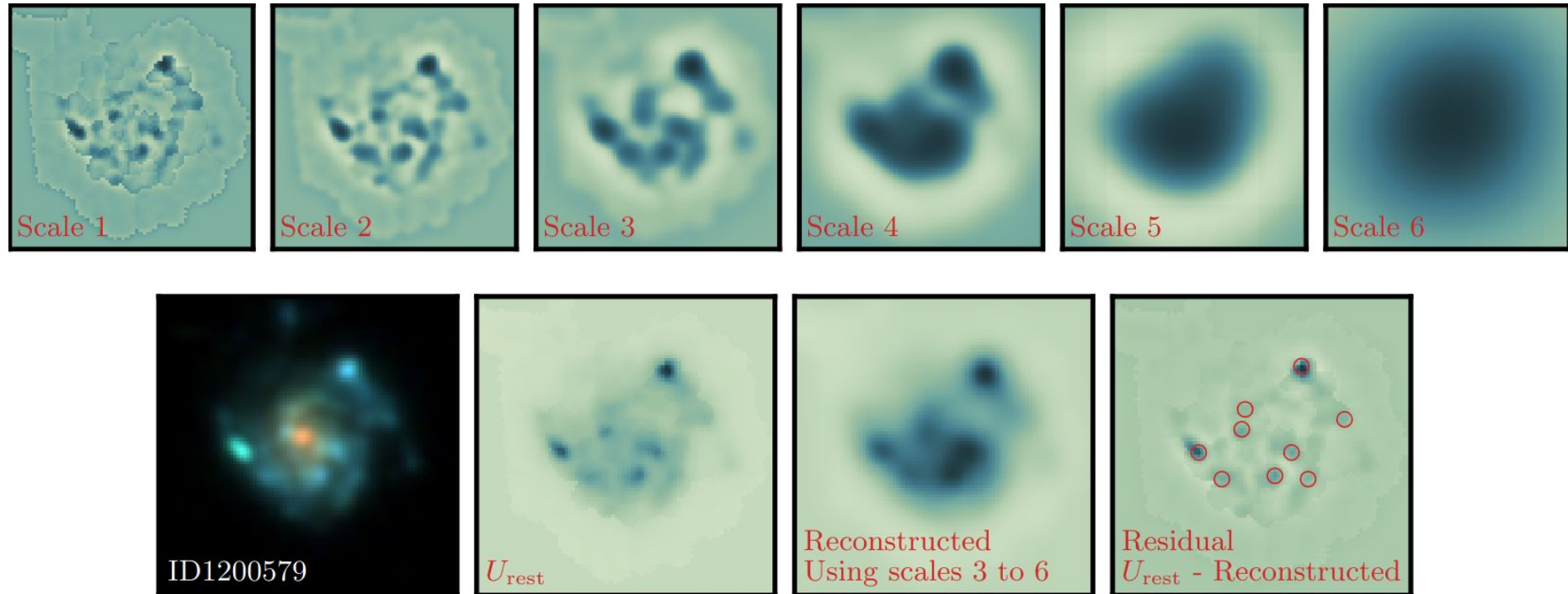
Clumps identification through starlet wavelet transform:
- The rest-frame U image decomposed into multiple spatial scales.
- Clumps are identified using a peak finding algorithm on the high-contrast image (marked by red circles)

SF evolution
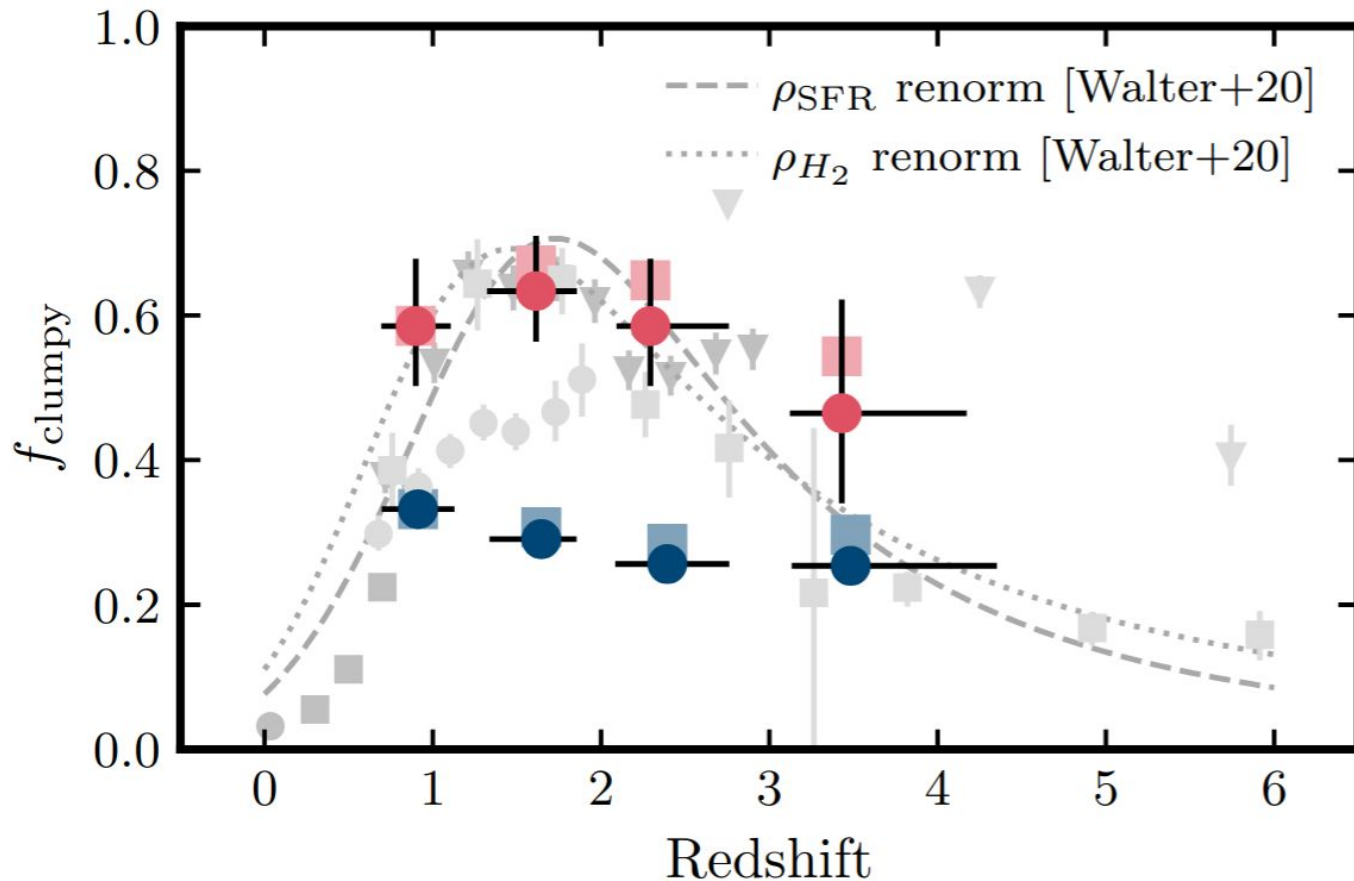
- Massive galaxies log(M∗/M☉) ≥ 10 exhibit a stronger evolution with z than low mass galaxies (8.5 < log(M∗/M☉) < 10).
- Clumpy fraction for massive galaxies peaks at around 60% near z ~ 2 and remains at around 40% at z ~ 4.
- For less massive galaxies, the clumpy fraction is observed to be at 30% for all redshif bins.

SF evolution

Galaxies at the peak of SFH have clumpy, irregular morphologies, with median masses of 10^7 M_o, SFR > 0.5 M_o/yr and sizes ~30–300 pc (Shibuya+16).

The Stellar Mass and Age Distributions of Star-Forming Clumps at $0.5 < z < 5$ in JWST CANUCS: Implications for Clump Formation and Destruction

VISAL SOK [ID],[1] ADAM MUZZIN [ID],[1] VIVIAN YUN YAN TAN [ID],[1] YOSHIHISA ASADA [ID],[2,3] MARUŠA BRADAČ [ID],[4,5]
VINCE ESTRADA-CARPENTER [ID],[6,7,8] KARTHEIK G. IYER [ID],[9,10] NICHOLAS S. MARTIS [ID],[4] GAËL NOIROT,[11]
GHASSAN T. E. SARROUH [ID],[1] MARCIN SAWICKI [ID],[8] CHRIS J. WILLOTT [ID],[12] SUNNA WITHERS [ID],[1]
SAMANTHA C. BEREK [ID],[13,2,14] AND KATHERINE MYERS [ID][1]

ABSTRACT

We investigate the resolved properties of star-forming clumps and their host galaxies at $0.5 < z < 5$ in the JWST CANUCS fields. We find that the fraction of clumpy galaxies peaks near $z \sim 2$ for galaxies with masses of $\log(M_{g,*}/M_\odot) \geq 10$. Galaxies with masses of $8.5 \leq \log(M_{g,*}/M_\odot) < 10$ show lower clumpy fractions with little redshift evolution. We identify and measure individual clump masses, finding that the aggregated clump stellar mass function (cSMF) follows a power-law slope of $\alpha = -2$ across all redshift bins, broadly consistent with in-situ clump formation. However, when split by galaxy mass, the cSMF is found to be flatter ($\alpha \sim -1.6$) for massive galaxies and steeper ($\alpha \sim -2.3$) for lower mass galaxies, with little redshift evolution. We further explore how clump formation and disruption mechanisms shape the cSMF. In particular, we find that the cSMF slope is flatter with increasing inferred gas fraction in younger clump populations (< 300 Myr), suggesting that gas availability favors the formation of more massive clumps. Alternatively, many high-redshift galaxies in our sample have disturbed morphologies and simulations show that clumps of ex-situ origins are comparably more massive to in-situ clumps, which can flatten the cSMF. We also examine clump evolution, finding the cSMF slope become flatter as clumps evolve and age. We interpret this as an indication of the long-term survivability of massive clumps, where feedback mechanisms preferentially disrupt low-mass clumps. Overall, the galaxy-mass dependent cSMF and age distribution point to a complex history for clumps, involving different and competing mechanisms for their formation and destruction.

SF evolution

High-z

Galaxies tend to be more clumpy and irregular in appearance compared to galaxies in the local universe.

Why?

More factors:

- Higher gas fractions
- More turbulent gas dynamics
- Less efficient feedback processes, regulating star formation and smoothing galaxy's appearance.

Low-z

The fraction of galaxies with clumpy morphologies decreases with decreasing redshift: galaxies in the local universe have smooth, and regular structures compared to high-z galaxies.

Why?

Feedback processes (supernova explosions, AGN) have more time to operate and regulate the gas and star formation in galaxies.

SF evolution

ALMA observations shows that the bulk of star formation in z~1−3 main sequence galaxies is in giant clumps, scaled versions of HII regions in local Universe.

- The velocity dispersion in GMC increases for clouds forming in gas with high external pressures and densities, i.e. starbursts, centres of galaxies, and high-redshift systems.
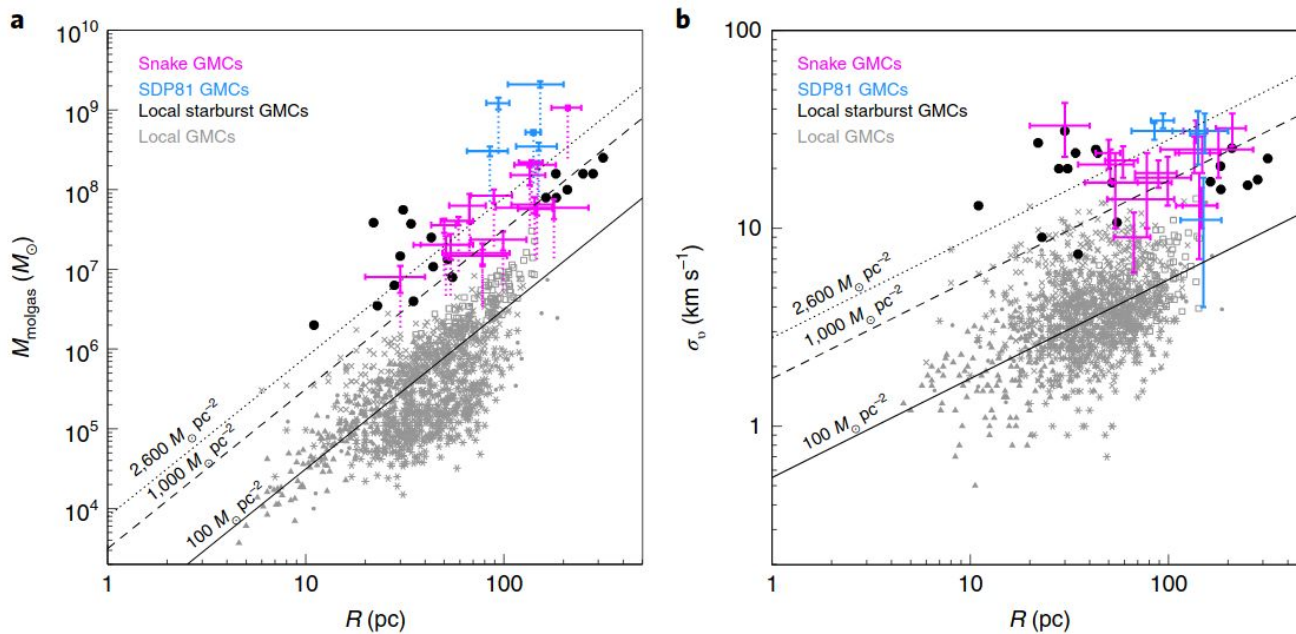
Fig. 1 Larson scaling relations from Dessauges-Zavadsky et al. (2019). Molecular gas masses (left panel) and internal velocity dispersions (right panel) are shown as a function of the size for a sample of clouds identified in the Cosmic Snake galaxy at $z \sim 1$ (pink; Dessauges-Zavadsky et al., 2019), in the SDP81 star forming galaxy $z \sim 3$ (blue; Swinbank et al., 2015), in local starburst galaxies (black) and in local quiescent galaxies (grey; see full list of references in Dessauges-Zavadsky et al., 2019). The black lines show fixed molecular gas mass surface densities of $100\,\mathrm{M_\odot\,pc^{-2}}$, $1000\,\mathrm{M_\odot\,pc^{-2}}$ and $2600\,\mathrm{M_\odot\,pc^{-2}}$. High redshift and local starburst galaxies show on average GMCs with larger surface densities, achieving energy equipartition at larger internal velocity dispersions.

The physics of GMC

Within molecular clouds there is a balance between self-gravity and thermal pressure. The physical parameters characterizing such a system are the Jeans length (λ_J), and the Jeans mass (M_J), assuming a spherical simmetry.

$$\lambda_J = \left(\frac{\pi c_s^2}{G\rho}\right)^{1/2} \sim 2.2 \text{ pc} \left(\frac{c_s}{0.2 \text{ km sec}^{-1}}\right) \left(\frac{n}{10^2 \text{ cm}^{-3}}\right)^{-1/2}$$

and

$$M_J = \frac{4\pi}{3}\rho\left(\frac{\lambda_J}{2}\right)^3 \sim 34 \, M_\odot \left(\frac{c_s}{0.2 \text{ km sec}^{-1}}\right)^3 \left(\frac{n}{10^2 \text{ cm}^{-3}}\right)^{-1/2},$$

Where:

c_s = is the sound speed

G = the gravitational constant

ρ = gas density

n = gas number density.

The physics of GMC

The minimum duration of the collapse because of self-gravity only is given by the free-fall time:

$$t_{\text{ff}} = \sqrt{\frac{3\pi}{32G\rho}} = \sqrt{\frac{3}{32}}\frac{\lambda_{\text{J}}}{c_s} \sim 3\,\text{Myr}\left(\frac{n}{10^2\,\text{cm}^{-3}}\right)^{-1/2}$$

Previous equations indicates that as collapse proceeds, the density increases and the Jeans parameters (length and mass) decrease, inducing fragmentation of the collapsing cloud.

Such fragmentation should stop once the gas ceases to behave isothermally. This occurs at large volume densities, when the gas becomes optically thick.
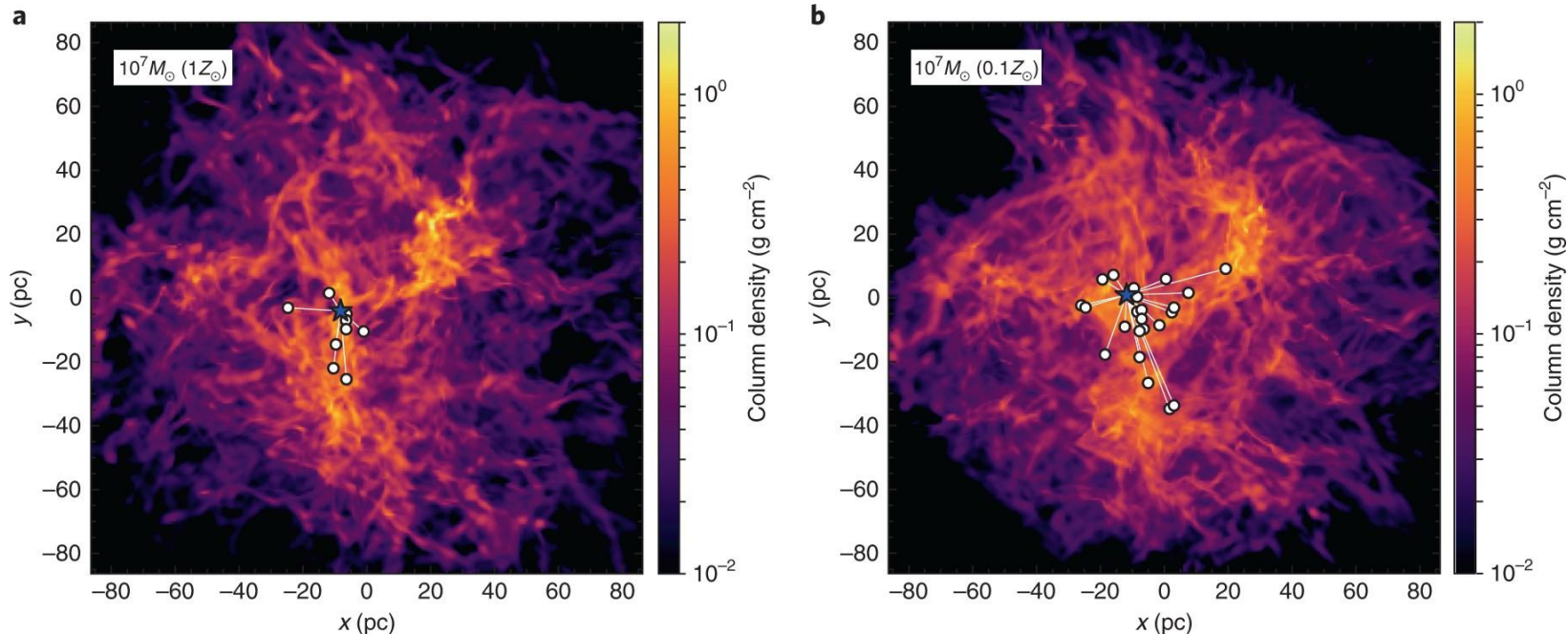
SF Efficiency

Fraction of gas converted into stars per unit time. It measures how efficiently a galaxy is able to convert its available gas into stars.

It can be calculated comparing SFR with the gas mass of a galaxy (using tracers such as H-alpha emission for the SFR and CO for the molecular gas).

The SFE is usually expressed as a percentage, and vary widely depending on the physical conditions of the gas: density, temperature, and metallicity, as well as the environment.

The SFE vary over time within a galaxy, depending on the availability of gas and the efficiency of feedback processes that regulate star formation.

SF Efficiency

Assuming that all the molecular clouds in our Galaxy are self-gravitating, collapsing then in a free-fall time, we can estimate the "free-fall rate" of star formation (SFR_{ff}) in the Milky Way

IMP = We are assuming that the only effect acting in the cloud is the self gravitation.

The molecular gas mass in our Galaxy, from ^{12}CO observations, is ~$10^9 M_o$ (Bolatto et al., 2013), and the typical free-fall time of molecular clouds is ˜10 Myr.
If all the gas is converted to stars within a free-fall time → SFR_{ff}~100 M_o/yr.
The observed SFR in MW and in nearby spiral galaxies is about a factor 100 times smaller than the typical free-fall rate.

The Star Formation Efficiency (SFE) is ~0.01.
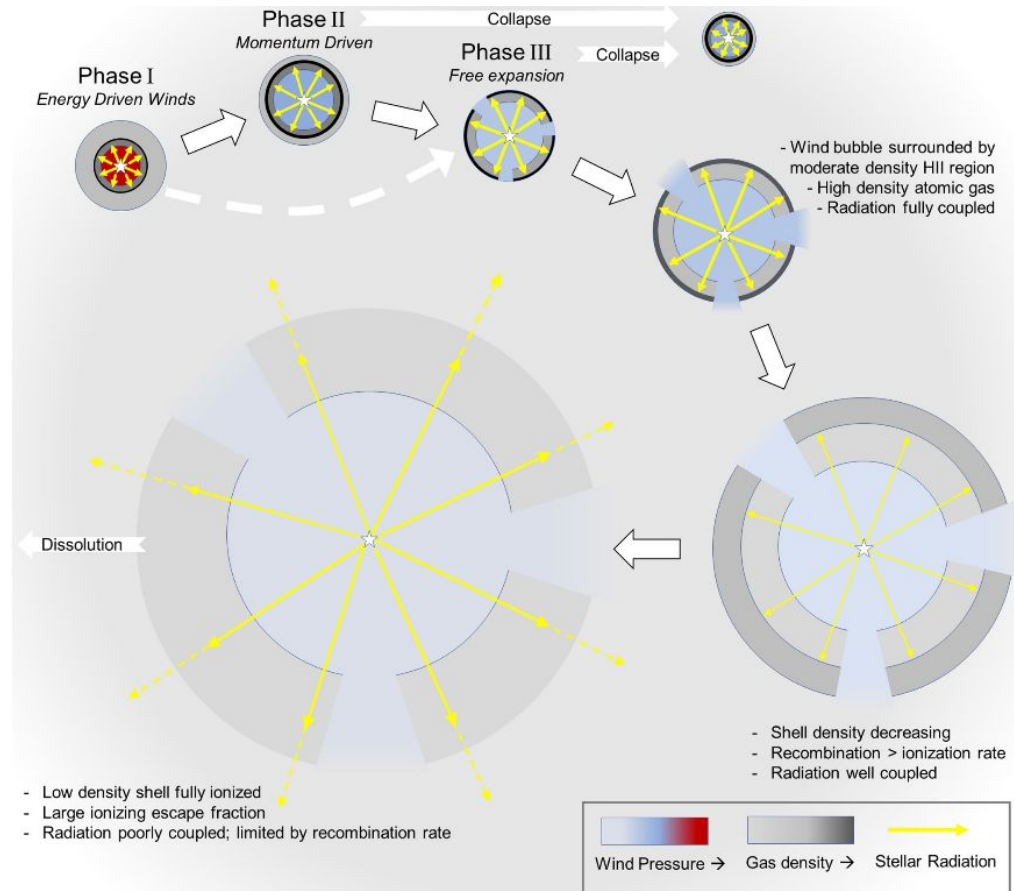
Rahner+17

SF Efficiency

This difference is due to the fact that not all gas is converted into stars, implying low SFE, or the timescale of star formation is much longer than the free-fall time?

SF Efficiency

This difference is due to the fact that not all gas is converted into stars, implying low SFE, or the timescale of star formation is much longer than the free-fall time?

Fig. Caption: SFE per free-fall time (median and 16th–84th percentile range) in a sample of nearby galaxies, as a function of galaxy stellar mass. The red data points are calculated using a constant value of the CO-to-H2 conversion factor (α_{CO}), while the grey data points are calculated using a metallicity-dependent α_{CO}.

Utomo+18
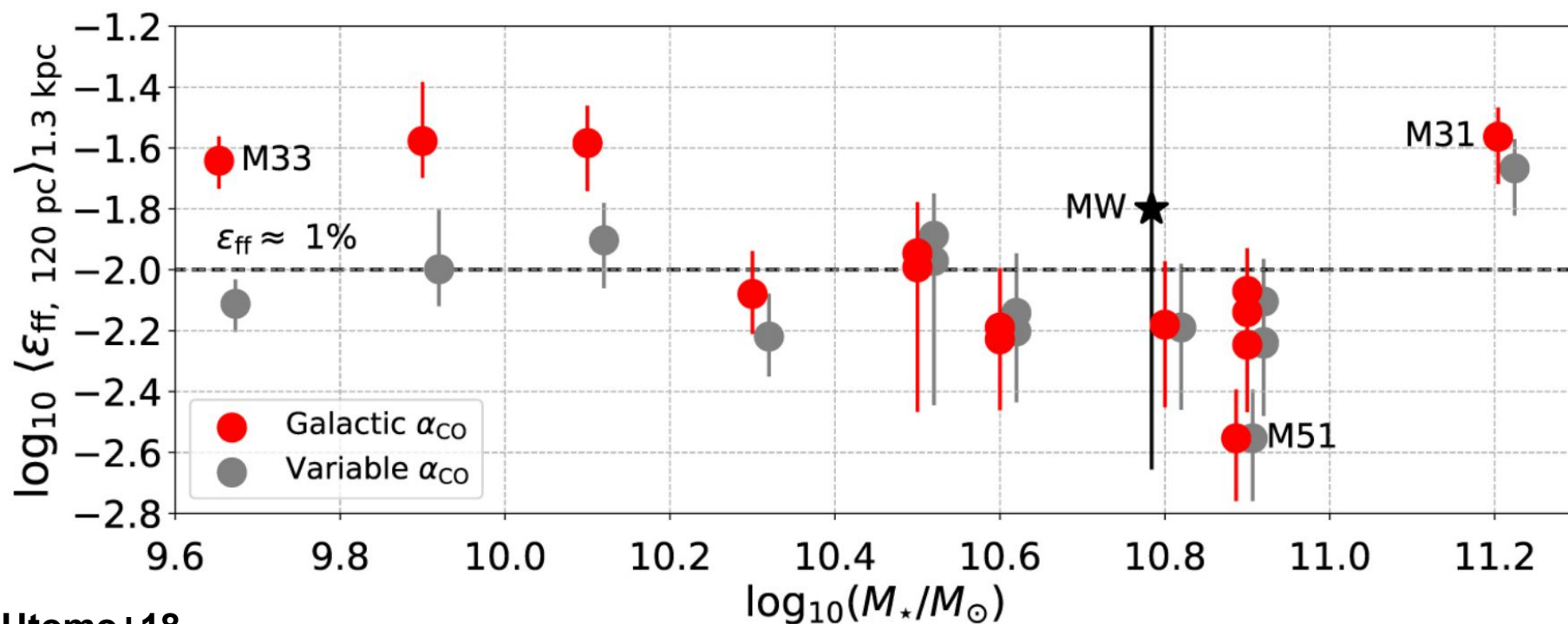
GMC timescale

Measurements of the GMC timescale is fundamental to answer these questions:

1. What is the lifetimes of GMCs as a function of the galactic environment?
2. What is the time necessary to disperse a GMC because of stellar feedback?

This can help to understand why SFE is only ~1%:
- GMCs live for many dynamical times and are efficient to convert gas into stars (they are just slow)
- GMCs live for one or few dynamical times, reaching low SFEs.

These cases are quite straightforward to distinguish observationally:

- If feedback operates slowly and GMCs are long-lived, the tracers of molecular gas and massive star formation will be co-spatial on cloud scale.

- If molecular gas and massive stars are distinct evolutionary phases of a rapid lifecycle, then the tracers should not be correlated.
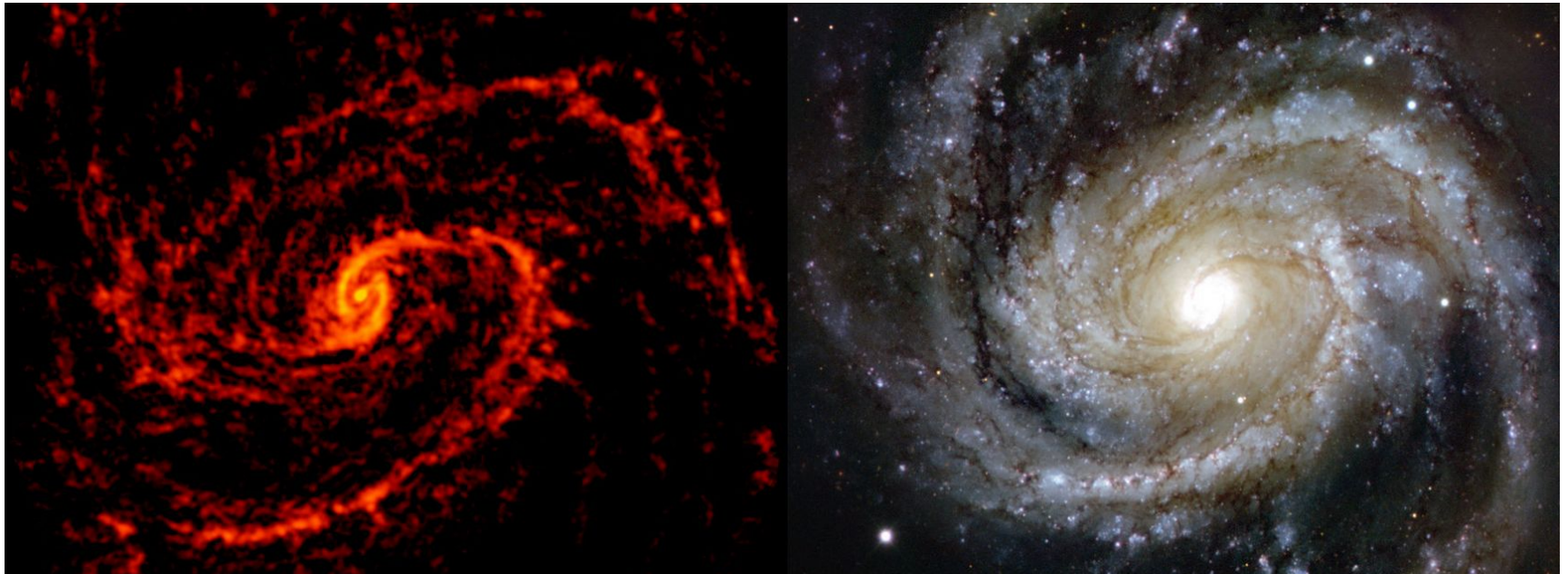
GMC timescale

ALMA observations can reach resolutions of 50–100 pc across the nearby galaxy population out to 20 Mpc, both for molecular gas traced by CO and massive star formation traced by Hα or ultraviolet emission.

This is essential complement to CO data, providing an absolute 'reference timescale'.
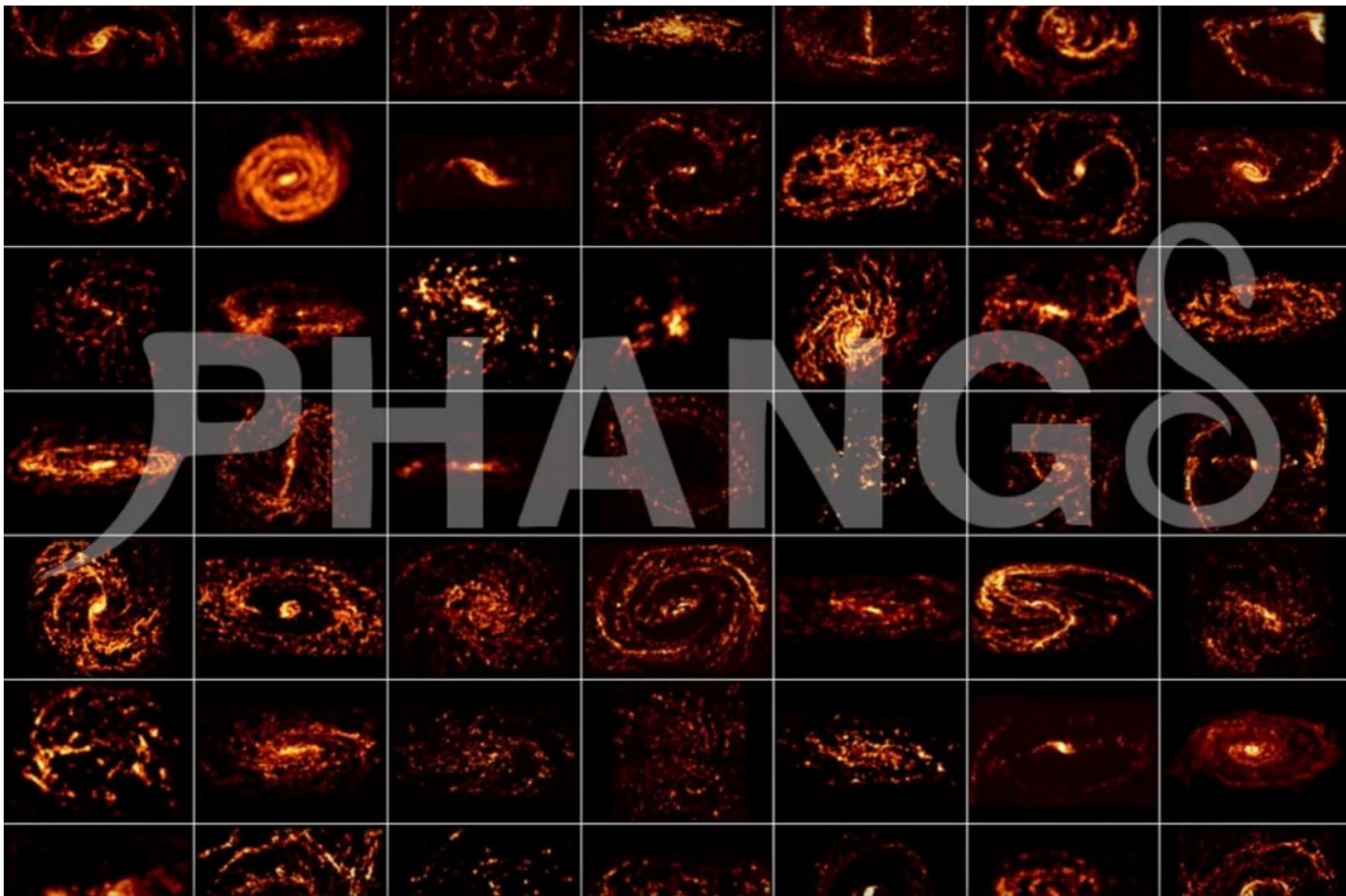
GMC timescale

High-resolution observations of gas and star formation in nearby galaxies show that CO and Hα emission rarely coincide on the cloud scale. Using empirical relation Kruijssen et al. (2019) and Chevance et al. (2020) estimated the GMC lifecycle in the nearby flocculent spiral galaxy NGC300 and to nine nearby star-forming spiral galaxies.
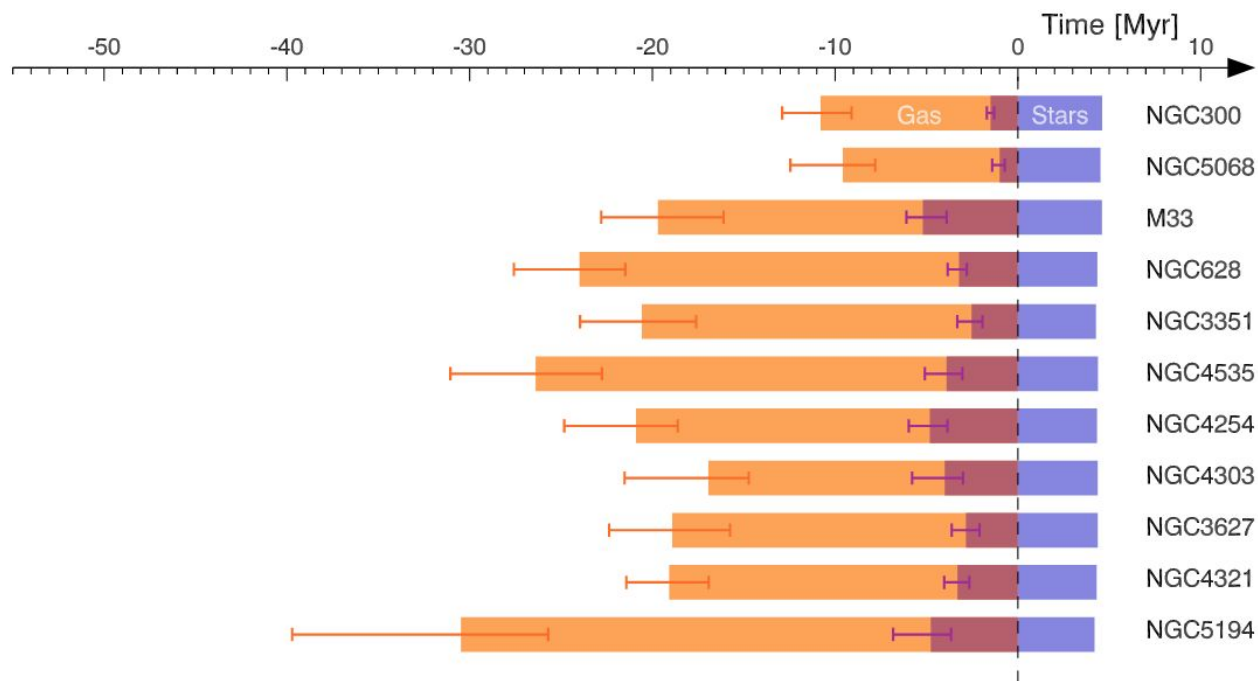
Fig. 7 Evolutionary timeline of the GMC lifecycle from molecular gas to star formation and feedback, for a sample of eleven nearby galaxies. The first phase (in orange) indicates the duration of the 'inert' CO phase, without any signs of massive star formation. During the second phase (in maroon), gas and massive stars coexist. The third phase (in blue) represents the isolated young stellar phase, after the gas has dispersed and when only Hα emission is visible. Galaxies are ordered from top to bottom by increasing stellar mass. This diagram is based on Figure 4 of Chevance et al. (2020), with the addition of NGC300 (from Kruijssen et al., 2019b) and M33 (from Hygate et al., 2019).

1. SFR-Gas Fraction

2. SF evolution

3. The physics of GMC

4. Star Formation Efficiency (SFE)

5. GMC timescale